Published in final edited form as:
Nat Struct Mol Biol. 2012 December ; 19(12): 1234–1241. doi:10.1038/nsmb.2438.

Structure of the pre-60S ribosomal subunit with nuclear export factor Arx1 bound at the exit tunnel

Bettina Bradatsch[1,6], **Christoph Leidig**[2,6], **Sander Granneman**[3,5], **Marén Gnädig**[1], **David Tollervey**[3], **Bettina Böttcher**[4,5], **Roland Beckmann**[2], and **Ed Hurt**[1]

[1]Biochemistry Center, Universität Heidelberg, Heidelberg, Germany.

[2]Department of Biochemistry, Gene Center and Center for Integrated Protein Science, Ludwig-Maximilians-Universität München, Munich, Germany.

[3]Institute of Cell and Molecular Biology, University of Edinburgh, Edinburgh, UK.

[4]European Molecular Biology Laboratory (EMBL), Heidelberg, Germany.

Abstract

Pre-ribosomal particles evolve in the nucleus through transient interaction with biogenesis factors, before export to the cytoplasm. Here, we report the architecture of the late pre-60S particle purified from *Saccharomyces cerevisiae* through Arx1, a nuclear export factor with structural homology to methionine aminopeptidases, or its binding partner Alb1. Cryo-electron microscopy reconstruction of the Arx1-particle at 11.9 Å resolution reveals regions of extra densities on the pre-60S particle attributed to associated biogenesis factors, confirming the immature state of the nascent subunit. One of these densities could be unambiguously assigned to Arx1. Immuno-electron microscopy and UV cross-linking localize Arx1 close to the ribosomal exit tunnel in direct contact with ES27, a highly dynamic eukaryotic rRNA expansion segment. The binding of Arx1 at the exit tunnel may position this export factor to prevent premature recruitment of ribosome-associated factors active during translation.

Ribosomes are key components of the cellular infrastructure that catalyze protein synthesis. They are evolutionary conserved throughout all kingdoms of life - bacteria, archaea and eukaryotes. However, eukaryotic organisms have evolved a sophisticated synthesis and assembly pathway for their 60S and 40S ribosomal subunits, which consist of four ribosomal RNA species (25S, 5.8S, 5S, and 18S rRNA, respectively) and about 80 ribosomal proteins (r-proteins). Ribosome assembly involves a myriad of eukaryote-specific biogenesis factors (between 150-200). In addition, nucleocytoplasmic transport through the nuclear pore complexes (NPCs) is necessary because the nuclear envelope separates the nucleoplasm, where most of the ribosomal assembly takes place, from the cytoplasm, where

Correspondence should be addressed to E.H. (ed.hurt@bzh.uni-heidelberg.de)..
[5]Present addresses: Centre for Synthetic and Systems Biology, University of Edinburgh, Edinburgh, UK (S.G.); School of Biological Sciences, University of Edinburgh, Edinburgh, UK (B.Bö.).
[6]These authors contributed equally to this work.

AUTHOR CONTRIBUTIONS B.Br. designed and performed the experiments and wrote the manuscript; C.L. performed the cryo-EM analysis supervised by R.B.; S.G. performed the CRAC experiments and the computational analyses in the laboratory of D.T.; M.G. performed some of the biochemical purifications and growth analysis; B.Bö. mediated knowhow and supplied EM facility for the negative stain EM; E.H. directed the project, designed experiments, and wrote the manuscript; all authors contributed to the interpretation of the results and helped write the manuscript.

ACCESSION CODES The cryo-EM reconstruction density map has been deposited in the Electron Microscopy Data Bank (EMDB) under accession code EMD-5513, atomic coordinates of the crystal structures modeled into the reconstruction can be found at the Protein Data Bank entry 3J2I.

COMPETING FINANCIAL INTERESTS The authors declare no competing financial interests.

Europe PMC Funders Author Manuscripts

the mature ribosomes function in translation[1,2]. The active transport channel of the NPC is formed by a meshwork of hydrophobic phenlyalanine-glycine (FG) rich repeat domains of a subgroup of nucleoporins. Transient interaction of transport receptors with these FG motifs allows passage of attached cargo through the transport channel[3]. Maturing pre-60S subunits are huge, hydrophilic particles of >2.5 MDa and their efficient translocation may therefore pose particular problems and require a special effort.

Although the nuclear export of ribosomal subunits has been analyzed in detail[4], little is known about the architecture and composition of the exported pre-60S particles compared to mature 60S subunits. Three-dimensional structures of mature eukaryotic ribosomes were revealed during the last decade by modeling of structures into cryo-electron microscopy (cryo-EM) reconstructions and, recently, by solving crystal structures of complete 80S ribosomes and separate 40S or 60S subunits[5-9]. Various pre-60S particles have been isolated via associated biogenesis factors as bait proteins and their composition has been determined[10]. Few ribosomal precursor particles have been analyzed by EM and factors on the surface have been mapped. Examples include analyses of pre-40S particles and localization of associated factors by cryo-EM[11,12], and analyses of pre-60S intermediates by negative stain EM with localization of several ribosomal and non-ribosomal proteins by immuno-EM[13,14].

Here, we focus on a late pre-60S particle that is associated with the biogenesis factor Arx1, which is located both in the nucleoplasm and cytoplasm. This particle is thought to represent an export intermediate, since it carries several nuclear export factors. One of them is the essential export adaptor Nmd3 that contains a nuclear export signal (NES) recognized by Crm1 (also known as exportin1 or Xpo1), the general nuclear export receptor for NES carrying cargo, in concert with RanGTP[15,16]. When re-bound to the isolated mature 60S subunit, Nmd3 was found to be located at the interface of the 60S subunit close to the r-protein Rpl10 by cryo-EM[17]. Another export receptor of the 60S subunit is the Mex67-Mtr2 heterodimer, which has been suggested to be recruited to double-stranded RNA, possibly to the 5S rRNA[18,19]. In addition, Arx1 has been identified as a third export factor with unusual properties; it has a methionine aminopeptidase fold and can bind FG repeat nucleoporins, thereby mediating translocation through the FG repeat channel of the NPC[20,21]. Furthermore, Ecm1 was suggested to act in 60S subunit export, since it too can interact with FG repeats of the channel nucleoporins[22]. Several other factors have also been implicated in nuclear export of the 60S subunit including the HEAT-repeat protein Rrp12[23], and Npl3[24].

We sought to further characterize the Arx1-purified pre-60S particle to gain insight into the process of how the huge pre-60S subunit might translocate through the active transport channel of the NPC. Cryo-EM of the isolated pre-60S particle uncovered structural differences from the mature 60S subunit. Biochemical analysis, negative stain EM combined with immuno-labeling, and RNA-protein cross-linking revealed the position of Arx1 and other pre-60S factors on the nascent 60S subunit. The binding site of Arx1 was further determined on an earlier pre-60S particle (Rix1-particle) that is associated with Rea1 and the Rix1-complex, allowing the comparison of two successive nascent 60S subunits. Altogether, our data indicate that the pre-60S particle that exits the nucleus has not yet adopted its mature topology. A scattered distribution of these nuclear export factors on the surface of this pre-60S subunit could facilitate transport through the NPC.

RESULTS

Arx1 and Alb1 decorate the same late pre-60S particles

To gain insight into the architecture of pre-60S particles carrying nuclear export factors, we focused on Arx1. This factor forms a salt-resistant complex with Alb1 (**A**rx1 **l**ittle

brother)[20,25] and is stably associated with late pre-60S particles in the nucleoplasm and cytoplasm[26]. To determine whether Arx1 and Alb1 are indeed associated with the same pre-60S particles, we affinity-purified various nascent 60S subunits via different TAP-tagged non-ribosomal bait proteins from yeast expressing HA-tagged Alb1. These particles, which range from early nucleolar, intermediate nucleoplasmic to late cytoplasmic stages, contained the expected pre-ribosomal factors as revealed by SDS-PAGE and Coomassie staining (Fig. 1a). Western analysis indicated the presence of the known nuclear export factors Nmd3 and Mex67-Mtr2 in the Arx1-TAP purification. When we analyzed Alb1-HA, we detected it in the same pre-60S particles that also contained Arx1, consistent with the model that Arx1 directly binds to the pre-60S subunit, and that Alb1 is recruited to the particle by Arx1[20].

These data also suggested that Arx1 and Alb1 are bound to intermediate nucleoplasmic particles associated with Rix1 and Nug1, but not to earlier nucleolar pre-60S particles that carry Ssf1 or Nsa1. In contrast, the export factors Nmd3 and Mex67-Mtr2 are absent from the Rix1-associated particles, but strongly enriched in the Arx1-associated particles (Fig. 1a). To confirm that Arx1 is a *bona fide* component of the Rix1-associated particle, we generated yeast strains expressing either integrated Rix1-TAP, Sda1-TAP or Lsg1-TAP, together with Arx1-Flag, and performed split-tag affinity purifications. Via the ProtA-tag we affinity-purified the Rix1-TAP, Sda1-TAP and Lsg1-TAP proteins from cell lysates. We then passed the TEV-eluates over an anti-Flag peptide column to select for Arx1-Flag, followed by elution with Flag peptides. The different pre-60S particles associated with Rix1-TAP (nucleoplasmic), Sda1-TAP (nucleoplasmic), and Lsg1-TAP (cytoplasmic) each contained Arx1-Flag with similar stoichiometry to other co-purified biogenesis factors (Fig. 1b). We obtained comparable results when we purified Rix1-TAP, Sda1-TAP, and Lsg1-TAP, respectively, from yeast strains expressing Alb1-Flag (data not shown).

These data support the model that the Arx1-Alb1 heterodimer is recruited to a late stage of the maturing nucleoplasmic pre-60S subunit, but prior to the recruitment of Nmd3 and Mex67-Mtr2. Notably, Arx1-Alb1 are associated with nascent 60S subunits before (Rix1) and after (Lsg1) nuclear export, strongly indicating that they are exported in association with the pre-60S particles. In contrast, other biogenesis factors such as Rix1, Rea1, Rsa4, or Lsg1, which all co-precipitate Arx1, are restricted to more distinct biogenesis intermediates, which are considered either exclusively nucleoplasmic (Rea1, Rsa4) or cytoplasmic (Lsg1).

Cryo-EM of the Arx1-particle shows the immature 60S subunit

To visualize the structure of the Arx1-particle, we performed cryo-EM single-particle analysis, using Alb1-TAP affinity-purified pre-60S subunits. Comparison of the cryo-EM reconstruction of the Arx1-particle at 11.9 Å resolution (see Supplementary Fig. 1a for Fourier shell correlation plot) with the reconstruction of a mature 60S subunit revealed substantial additional mass in several areas of the Arx1-particle (Fig. 2a, Supplementary Fig. 1b). A globular density (red) is situated directly in front of the ribosomal exit tunnel and a large bulky density (orange) is located at the common helix of the 3′-end of the 5.8S rRNA and the 5′-end of the 25S rRNA. Also the central protuberance region is surrounded by additional mass forming an elongated shape (yellow) and a triangular density is visible in the center of the intersubunit surface (green). An elongated density (cyan) extends from the stalk base to the E-site, blocking access to all of the tRNA binding sites and the peptidyl transferase center (PTC). Furthermore, a globular shape (blue) is observed at the translation factor binding site and a chain-like density (purple) extends from this position along the surface of the pre-mature subunit towards the exit tunnel.

In negative stain EM combined with single particle analysis, Arx1-TAP and Alb1-TAP affinity-purified particles each classify into three comparable main orientations with

characteristic structures, the *foot*, *knob* and *nose* (Supplementary Fig. 2; for composition, see also Fig. 1a). Characterized by these common features, we will refer to these particles collectively as the "Arx1-particle". The cryo-EM structure of the Arx1-particle was readily reconciled with the negative stain class averages, suggesting that the *foot*, *knob*, and part of the *nose* structure are possibly formed by pre-ribosomal factors (Fig. 2b) or may contain rRNA not finally processed or not yet in its final conformation (see Discussion).

Overall, the structures of the mature 60S subunit that were previously determined by cryo-EM[6] and x-ray crystallography[27] nicely fit into the electron density observed for the pre-mature 60S subunit in our reconstruction of the Arx1-particle (Fig. 2c and data not shown), indicating that maturation is rather complete for most parts of the subunit. However, several features of the pre-60S particle still differ from the mature subunit (Supplementary Fig. 1b). The most obvious rearrangement is observed in the region of the central protuberance. The 5S rRNA and helix 38 (A-site finger) of the 25S rRNA cannot be clearly recognized at their final positions in the Arx1-particle (Fig. 2c). Also, the late-joining r-protein Rpl10 that is located between the central protuberance and the stalk base in the mature subunit seems not to be present in the pre-60S structure. The density found at the mature location of Rpl10 does not fit the shape of the r-protein. Moreover, the electron density observed in this position appears to represent RNA rather than protein, because it displays typical features of RNA density: good visibility at high contour level and helical twist (Fig. 2c). It is possible that the A-site finger may be rearranged to occupy this space. Another rearranged structural feature of the 60S subunit is helix 69 of the 25S rRNA, located in the center of the intersubunit surface where it is involved in the formation of two intersubunit bridges[27]. While it points towards the A-site in the mature subunit, it is turned by almost 180° in our reconstruction, now pointing towards the E-site (Fig. 2a, top row). Furthermore, we did not observe any density for the P-stalk in our reconstruction and we found that the stalk base was different from the mature subunit in the region of P0 (Supplementary Fig. 1b). In addition to P1 and P2 that were clearly absent, Rpl12, which forms the base of the stalk together with P0, appeared also to be absent from the nascent 60S subunit.

Taken together, our reconstruction of the Arx1 particle provides the first cryo-EM map of a pre-60S subunit. This structure underscores the immature stage of the nascent subunit and reveals a number of extra electron densities that could correspond to bound ribosome biogenesis factors (see below).

Localization of biogenesis factors on the Arx1-particle

To assign pre-ribosomal proteins to the extra densities observed in our cryo-EM reconstruction of the Arx1-particle, we determined the location of selected HA-tagged r-proteins and ribosome biogenesis factors on Alb1-TAP purified particles. Complementation assays showed the functionality of the HA-tagged proteins (Supplementary Fig. 3a). We used anti-HA antibodies to generate an additional mass in close proximity to the respective HA-tagged proteins, allowing visualization by negative stain EM. In parallel, we analyzed the efficiency of antibody labeling by SDS-PAGE and Coomassie staining (Supplementary Figure 3b). We labeled Rpl3-HA and Rpl5-HA, which were previously localized on the Rix1-particle[14], with the anti-HA antibody on the Arx1-particle (Fig. 3a). Rpl5 localized to the region of the *nose* structure, supporting our conclusion that the *nose* might represent part of the central protuberance. Immuno-labeling of Rpl8 and Rpl26 on the Arx1-particle allowed comparison of the Arx1-particle to the atomic structure of the mature 60S subunit (Fig. 3a, Supplementary Fig. 3c, d).

We observed the antibody signal for immuno-labeled Arx1-HA in the immediate vicinity of the *knob* structure (Fig. 3a). We identified the *knob* structure as the additional density observed directly at the ribosomal exit tunnel in our cryo-EM reconstruction of the Arx1-

particle (red density, Fig. 2a, b). Consistently, the crystal structure of the human Arx1 homolog Ebp1[28,29] fits well into this part of the cryo-EM map (Fig. 3b). The Ebp1 structure leaves parts of the density empty, however, Arx1 is larger than Ebp1 (64 kDa vs. 44 kDa due to loop insertions) and some of the density may also belong to Arx1's much smaller binding partner Alb1 (19 kDa). Notably, the observed density appears smaller than expected for the complete Arx1-Alb1 heterodimer (83 kDa). Missing density can be explained, however, by possible flexibility of Alb1 or the loop insertions in Arx1 of yeast. These results indicate that the density observed in front of the ribosomal exit tunnel represents Arx1, possibly together with Alb1.

The ribosome biogenesis factor Tif6 prevents premature subunit joining and was found to bind to the intersubunit surface of mature 60S subunits, contacting Rpl23, Rpl24, and the sarcin-ricin rRNA loop[9,30]. The non-ribosomal density observed at exactly this position in our cryo-EM reconstruction (blue density, Fig. 2a, b) matches Tif6 in size and shape and the crystal structure of Tif6[31] fits well into the density (Fig. 3c). Consistently, we found the antibody signal for Tif6-HA at the top of the particle (Fig. 3a). Taken together, these data indicate that the density labeled in blue represents Tif6, and confirm its location on the pre-mature 60S subunit.

The immuno-EM signal for Nsa2-HA localized to the top of the Arx1-particle, close to the signal for Rpl5 (Fig. 3a, Supplementary Fig. 3c, d). Nsa2 is a biogenesis factor that is required for processing of internal transcribed spacer 2 (ITS2) and, like Tif6, is already present in earlier particles[14,32]. Based on our immuno-labeling data, the cyan density stretching from the E-site to the stalk base in the Arx1-particle reconstruction might represent – or at least contain – Nsa2 (Fig. 2a, b and 3a). We also immuno-labeled HA-tagged Nmd3, Mex67, Mtr2, and Ecm1 on Alb1-TAP, but none of these proteins were efficiently labeled by the antibody as evaluated by SDS-PAGE and Coomassie staining (see also Supplementary Figure 3b) and thus were not further analyzed by EM (data not shown).

Taken together, immuno-labeling combined with negative stain EM revealed the relative positions of several biogenesis factors on the surface of the Arx1-particle and – together with the positions of marker r-proteins – allowed their assignment to additional densities observed on the Arx1 pre-60S particle reconstructed by cryo-EM.

UV cross-linking reveals Arx1 close to the exit tunnel

To experimentally determine where Arx1 contacts the surface of the pre-60S subunit, we applied the CRAC (UV **cr**oss-linking and **a**nalysis of **c**DNA) methodology previously used to successfully identify RNA-protein interactions in ribosomal subunits[33-35]. We found that Arx1 directly contacts several rRNA elements that cluster on the 60S subunit surface near the exit tunnel. In particular, Arx1 was efficiently cross-linked to helix 59 (expansion segment ES24) of the 25S rRNA as well as to ES27, an expansion of helix 63 of the 25S rRNA (Fig. 4a–c). Helix 59 was reported to contact the Sec61-complex within the ER membrane[36], whereas ES27 is a highly dynamic rRNA element with two major conformations, one pointing towards the L1-stalk (*in*), and the other reaching the peptide exit tunnel (*out*). ES27 is essential for ribosome biogenesis, possibly involved in pre-rRNA processing or in stabilization of mature rRNA[37]. In the mature ribosome, ES27 was suggested to coordinate recruitment of non-ribosomal factors (e.g. chaperons) to the exit tunnel, from which the nascent polypeptide chain emerges[6,36]. Arx1 is likely to contact ES27 in the *out* position close to the exit tunnel, because a simultaneous interaction with both, helix 59 and ES27, is possible only in this conformation (Fig. 4c). Consistently, analysis of the Arx1 binding site in our cryo-EM reconstruction using the high-resolution crystal structure of the mature 60S subunit showed that Arx1 contacts rRNA helix 59 (Fig. 4d), as well as ES27 in the *out* position (visualized only at lower contour levels; Fig. 4e).

Arx1 also contacts Rpl25 and Rpl35 and binds close to Rpl19 (Fig. 4d). Notably, due to low cross-linking efficiency, we could not determine reproducible cross-linking sites for Alb1. Similarly, we could not detectably cross-link Tif6 (Granneman, unpublished data). In conclusion, the CRAC data for Arx1 are in excellent agreement with the immuno-labeling results and its binding site observed in cryo-EM, supporting the model that Arx1 binds in proximity to the exit tunnel and hence could affect this hallmark structure of the ribosome during biogenesis (see Discussion).

Arx1 localizes to the *knob* structure of the Rix1-particle

Previous studies analyzed the Rix1-associated particle by negative stain EM and localized several non-ribosomal biogenesis factors (e.g. Rea1, Rix1, Rsa4) as well as r-proteins (e.g. Rpl5, Rpl3) on this nascent 60S subunit by immuno-labeling[13,14]. Since Arx1 is also present on the Rix1-particle (see above), we wanted to find out where it localizes on this intermediate with respect to the other factors. Hence, we affinity-purified Rix1-TAP from yeast expressing chromosomal Arx1-HA, followed by immuno-labeling using anti-HA antibodies (Supplementary Fig. 4a). We localized Arx1 to the knob-like structure on the top of the Rix1-particle, opposite the long protruding tail that corresponds to the huge AAA^+ ATPase Rea1 (Fig. 5a, b; Supplementary Fig. 4b, c). Thus, Arx1, likely together with Alb1, forms the knob-like protrusion that is a distinct structural landmark on the top of the Rix1-particle. This position is relatively close to r-protein Rpl3 and more distant from Rpl5 (Fig. 5b). Together, these data suggest that the *knob* structure represents the Arx1-Alb1 heterodimer in both the Rix1- and Arx1-particles.

The Arx1-TAP and Alb1-TAP particle preparations should include a subset of Rix1-associated particles, with a typical Rea1 tail (see above). We therefore performed a classification of the Alb1-TAP affinity-purified particles visualized by EM, and analyzed the distribution of the particles among the different classes. This quantitative analysis indicated that ~45% of the Alb1-TAP purified particles belong to the three main orientations (views 1–3) referred to as the “Arx1-particle”, whereas only 12% were classified as “Rix1-particle“ exhibiting the typical Rea1 tail (Supplementary Fig. 7). Interestingly, the overall morphology of “view 2“ Arx1-particles resembles a class of tail-less Rix1-TAP purified particles that was previously generated by ATP-treatment of purified Rix1-particles to release Rea1 and the Rix1-complex (Fig. 5c; see ref. 14). Thus, the Rix1-particle carrying Rea1, Rix1-complex and Rsa4 appears to be the precursor of the Arx1-particle, which lost these latter factors due to the action of Rea1[14] while recruiting new factors, which include the nuclear export factors Nmd3 and Mex67-Mtr2 (see Discussion).

DISCUSSION

Here we have analyzed the EM structure of pre-60S particles that contain the Arx1-Alb1 heterodimer. These are relatively late particles of the 60S biogenesis pathway that are eventually exported from the nucleus into the cytoplasm. On the one hand, Arx1-Alb1 is associated with a well-studied nucleoplasmic pre-ribosomal particle that carries the dynein-related AAA^+ ATPase Rea1 and the Rix1-complex (Rix1-particle). However, the major pool of Arx1-Alb1 associated pre-60S particles, termed the Arx1-particle, lack Rea1 and Rix1, and represent a biogenesis intermediate that follows the Rix1-particle. The Arx1-particle exhibits characteristic structures such as the *foot*, *knob*, and *nose*, which are prominent features seen both by negative stain and cryo-EM. We show for a few of these structures that they corresponded to additional non-ribosomal densities on the pre-60S particle absent from the mature 60S subunit. Employing immuno-EM, the positions of several ribosomal and non-ribosomal proteins could be mapped. To our knowledge, the Arx1-particle is the first immature 60S subunit precursor for which a cryo-EM structure has been determined.

In our reconstruction, the core of the Arx1-particle is similar to the mature 60S subunit, indicating a late assembly stage. However, several important functional sites of the mature 60S subunit are not yet fully developed on the Arx1-particle. Apparently, the flexible P-stalk is absent from the Arx1-particle. This structure is composed of ribosomal proteins P0 and acidic P1 and P2 on the mature 60S subunit. The P-stalk functions in recruiting translation factors to the GTPase center[38]. However, the stalk base seems to be under reconstruction in the Arx1-particle. Mrt4, a P0-paralog that requires the Yvh1 factor for its release from the 60S pre-ribosome[39,40], as well as Yvh1 and P0 are detected in the Arx1-particle by mass-spectrometry. On the other hand, P1 and P2 are known to be late joining r-proteins[41] that likely associate with cytoplasmic 60S subunits following release of Arx1-Alb1.

Moreover, the Arx1-purified pre-60S particle differs from the mature subunit in the region of the central protuberance. Together with the observed extra densities, the immature central protuberance gives rise to the characteristic *nose* structure of the Arx1-particle, suggesting that final conformational rearrangements of the central protuberance and/or release of ribosome biosynthesis factors from this region may not have yet occurred. The yellow extra density at the central protuberance (Fig. 2a, b) may contain part of the structures that form the central protuberance in the mature ribosome, e.g. 5S rRNA, Rpl5, and Rpl11. Possible ribosome biogenesis factors that could contribute to the yellow density are the Mex67-Mtr2 complex or the GTPase Nug1, both of which were shown to interact with 5S rRNA *in vitro*[18,42]. The pre-ribosomal factors responsible for the additional density in the pre-ribosomal structure, other than Tif6 and Arx1-Alb1, have not been unambiguously identified. The localization of the green shape (Fig. 2a, b) – albeit smaller – is similar to that found for MPB-tagged Nmd3 on the intersubunit surface of mature 60S in a previous cryo-EM study[17]. Interestingly, the purple density stretches far across the pre-ribosomal surface and contacts both Arx1 and the Tif6 density, thus possibly providing a means of direct crosstalk between the distant areas around the stalk base and the exit tunnel. This might enable communication of the state of maturation at the stalk base and the release of Arx1 at the exit tunnel. Likewise, the cyan density might coordinate and communicate the progression of maturation around the stalk base and the tRNA binding sites. Another biogenesis factor Rei1, implicated in release of Arx1-Alb1 from the subunit[25,43], might be represented by the purple density that also contacts Arx1. Other candidate proteins responsible for the extra densities are Ecm1 and several GTPases including Nog1, Nug1, Nog2, and Lsg1 (involved in the release of Nmd3[44]).

Notably, all these additional densities on the Arx1-particle were observed at functionally relevant sites of the 60S subunit, blocking access to the ribosomal peptidyl transferase center (PTC), the tRNA binding sites, the stalk base, the intersubunit surface and the exit tunnel. A recent study showed that biogenesis factors present on a late cytoplasmic pre-40S particle block all sites important for translation initiation[12]. Similarly, the positioning of biogenesis factors, as well as the immature state of important structures on the Arx1-particle are hindering untimely onset of translation. Furthermore, it was reported that final cytoplasmic pre-40S maturation involves a translation-like cycle[45]. It is possible that also pre-60S subunits engage in such a quality control checkpoint to assure functionality and final rRNA maturation and factor release. Together, these observations illustrate the multitude of control mechanisms that keep the nascent subunit from pre-mature engagement in translation during this advanced phase of maturation.

The prominent *foot* structure of the Arx1-particle is located above the region where the 3′-end of the 5.8S rRNA and the 5′-end of the 25S rRNA end in a common helix in the mature subunit. Arx1-associated particles mainly contain mature 25S and 5.8S rRNA. However, a small amount of 27SB pre-rRNA (in which the 3′-end of 5.8S and 5′-end of 25S rRNA are linked by ITS2) and some 7S pre-rRNA (in which the 3′-end of 5.8S rRNA is extended) are

also recovered. This indicates that C2 cleavage, which generates the 3′-end of the 7S pre-rRNA, has occurred in most Arx1-associated particles, but processing of 7S to the 5.8S rRNA has not yet taken place in all particles[26] (data not shown). This is in agreement with the reported cytoplasmic location of the final step in 5.8S rRNA processing[46]. The *foot* structure may therefore represent retained factors involved in processing and/or folding of ITS2 or it might protect this region and/or offer a binding platform for processing factors until nuclear export and/or maturation of this area are completed.

The position of the unconventional export receptor Arx1 could be unambiguously assigned to the characteristic *knob* structure observed on either the Rix1- or Arx1-purified 60S subunit particle. The *knob* structure is located directly in front of the exit tunnel and the observed binding site of Arx1 is in good agreement with an earlier suggestion that it may bind in close proximity to Rpl25[43]. The flexible rRNA expansion segment ES27 was suggested to be involved in regulating the access of non-ribosomal factors to the exit tunnel[36]. Binding of Arx1 to the pre-ribosome at the exit tunnel and interaction with ES27 might favor the ES27*out* conformation, which potentially facilitates nuclear export of the subunit. Arx1 is structurally related to methionine aminopeptidases (Met-APs), which remove N-terminal methionine from the nascent polypeptide chain; however, Arx1 lacks this enzymatic activity[20]. It is therefore plausible that Arx1 binds the pre-60S subunit in a similar manner and position to Met-AP on the mature 60S subunit. We speculate that Arx1 could function as a placeholder for Met-AP and/or other cytoplasmic translation-associated factors that bind to the exit tunnel. In this way, Arx1 could restrict the access of such factors to the exit tunnel region of the immature 60S subunit. This could avoid steric hindrance during export of the 60S subunit (note that Arx1 also acts as export factor; see below) or premature association of translation-competence. Last but not least, Arx1 may act as quality control factor to ensure correct assembly of this key site on the 60S subunit before the particle is exported to the cytoplasm.

Finally, the localization of the export factor Arx1 supports the model that transport receptors are distributed over different regions of the pre-60S subunit. The export adapter Nmd3 was found to interact with the intersubunit surface of the mature 60S subunit[17]. Mex67-Mtr2 was shown to interact with 5S rRNA *in vitro*[18] and may thus bind to the central protuberance at the “top” of the subunit. Arx1 binds close to the exit tunnel on the opposite side of the pre-60S subunit, a location that is very distant from the predicted interaction sites of the other two export factors. It might have been envisaged that nuclear export factors would be needed to initiate subunit export and then “tow” the subunit through the nuclear pore complex. However, the dispersed distribution of export factors on the pre-60S surface supports a view that no single region of the 60S subunit is sufficient for efficient passage through the nuclear pore. Rather, several export factors scattered over the complete surface of the pre-60S subunit are required to shield and efficiently export this huge cargo through the hydrophobic FG repeat phase of the nuclear pore into the cytoplasm.

Online Methods

Yeast strains

Yeast strains used in this study are listed in Supplementary Table 1. The genotype of the DS1-2b strain is MATalpha his3-Δ00 leu2-Δ1 trp1-Δ63 ura3-Δ52 derived from FY23xFY86[26]. TAP-tag or 3HA-tag were genomically integrated at the C-terminus as described[49,50]. For genomic integration of the Flag-tag the sequence of the Flag-epitope was integrated into the F3 primer[50]. For genomic integration of C-terminal His_6-TEV-ProtA-tag the integration cassette plasmid pFA6a-HTpA-HIS3MX4 (kindly provided by D. Kressler) was used.

CRAC analysis of Arx1

The CRAC method and bioinformatics analysis were performed as described[35] using the Arx1-HTP (His_6-TEV-ProtA) strain for CRAC analysis of Arx1 and the parental strain DS1-2b as a negative control. Two independent experiments were performed and the results merged.

Biochemical purification of pre-60S particles

Particles were essentially purified from 2-4 liters YPD liquid cultures grown to log phase at 30°C via TAP (tandem affinity purification) in standard buffer (50 mM Tris-HCl [pH 7.5], 100 mM NaCl, 1.5 mM or 5 mM $MgCl_2$ [where indicated], 0.075 % (v/v) NP-40) as described[26] with the following modifications. NP-40 was present only during cell lysis. Final eluates were in standard buffer without NP-40, with 0.5 mM DTT and 3.5 mM EGTA.

For split-tag purifications the TEV-protease eluate from the first affinity purification step of a TAP purification exploiting the ProtA-tag present on the bait protein was applied to anti-Flag M2-agarose from mouse (Sigma) for 1 hour at 4°C, followed by elution for 45 minutes at 4°C with 3xFlag peptide (Sigma) in standard buffer without NP-40 with 0.5 mM DTT.

Immuno-labeling, negative stain EM, single particle analysis and random conical tilt

Anti-HA antibody (monoclonal HA.11, Covance) was present in 1:50 (used for negative stain EM) or 1:200 dilution during the incubation on Calmodulin beads. Binding time was extended to 1.5 hours at 4°C. The tandem affinity-purified, split-tag purified, or TAP-purified and immuno-labeled particles were negatively stained with 2% uranyl acetate using the sandwich technique, imaged under low dose at 200 kV at 27,500 fold magnification (5.2 Å/pixel) with a Philips CM200 FEG transmission electron microscope supplied with a 2k x 2k CCD camera (TVIPS-GmbH) or at 100 kV at 33,000 or 53,000 fold magnification (3.6 Å/pixel or 2.2 Å/pixel) with a Philips CM120 BioTWIN LaB6 cathode transmission electron microscope supplied with a 4k x 4k CCD camera (FEI slow scan; used for negative stain of Fig. 4), all essentially as described[14]. Boxing of particles using "Boxer"[51] and image processing using IMAGIC-5[52] for single particle analysis were also essentially done as described[14].

For random conical tilt[53], micrographs were taken at 0° and −55° tilt using the CM200 FEG microscope. A map was calculated from the tilted particles belonging to one class of untilted particles using IMAGIC-5[53] and SPIDER[54] software and displayed using the UCSF Chimera[55] software.

Image and particle numbers analyzed were 176/4201 for Arx1-TAP, 250/8449 for Alb1-TAP Arx1-HA without anti-HA, 201/5236 for Alb1-TAP Rpl3-HA, 213/3310 for Alb1-TAP Rpl5-HA, 259/5933 for Alb1-TAP Rpl8-HA, 224/4331 for Alb1-TAP Rpl26-HA, 200/3835 for Alb1-TAP Arx1-HA, 162/4983 for Alb1-TAP Nsa2-HA, 116/3216 for Alb1-TAP Tif6-HA, 200/1476 for Rix1-TAP Arx1-HA, 170/2141 for Rix1-TAP, all with anti-HA, and 55/7219 for Alb1-TAP, all at 1.5 mM $MgCl_2$, and 60/11,922 for Alb1-TAP at 5 mM $MgCl_2$.

Cryo-EM and 3D-reconstruction

As previously described[56], samples were applied to carbon-coated holey grids, and micrographs were recorded under low-dose conditions (20 $e^-/Å^2$) on a Titan Krios TEM (FEI Company) microscope at 200 kV in a defocus range of 1.0–3.5 μm with a TemCam F416 camera (4,096 × 4,096 pixel, TVIPS GmbH) resulting in a pixel size of 1.049 Å on the object scale. The data were processed with the SPIDER software package[54]. Images were manually inspected for good areas and power spectra. Particles were automatically picked from 6,359 micrographs using projections of the crystal structure of the *S. cerevisiae* 60S

ribosomal subunit (PDB: 3O58[7]) as a template resulting in 222,229 particles. After initial alignment to the 60S ribosomal subunit, remaining non-ribosomal particles and 80S contaminations were removed by semi-supervised classification using iterative multi-reference 3D projection alignment. Templates were provided only for the initial classification step. Subsequently, the respective output maps of the previous classification rounds were used as new templates. Non-ribosomal particles were identified by their higher cross-correlation to an essentially featureless high-contrast density than to ribosomal references. An 80S-containing population of particles accumulated when the prominent orange-colored ligand was removed from the density and the resulting map was supplied as alternative reference during classification. 54,196 pre-ribosomal particles were then classified using maps of consecutive refinement rounds as templates. Using these quasi identical templates, the dataset was classified according to the most relevant intrinsic heterogeneity (e.g. density in the intersubunit space) minimizing the risk of introducing bias by artificial templates. Subsequently, the data were analyzed by focused sorting according to the density below the exit tunnel using a cylindrical binary mask (removing 6,795 particles)[47,57]. 8,322 particles were used for an initial reconstruction of the Arx1 pre-60S ribosomal particle at 14.3 Å resolution. In an effort to improve the reconstruction the entire data set was then re-processed. Considering the substantial additional mass identified on the pre-60S subunit in the previous reconstruction, this reconstruction was now used as template for the initial alignment. This increased the number of identified pre-ribosomal particles to 112,632. These particles were again classified using maps of consecutive refinement rounds as templates, resulting in a stable set of 63,943 particles that was used for reconstruction of the Arx1-particle. The final contrast transfer function corrected reconstruction has a resolution of 11.9 Å, based on the Fourier Shell Correlation with a cutoff value of 0.5. The density for the conserved 60S core and additional densities were isolated manually using the UCSF Chimera[55] software.

Miscellaneous

Antibodies used for Western analysis in the following dilutions were anti-HA 1:3,000 (HA.11 mouse monoclonal antibody, clone 16B12, Cat.-No. MMS-101R, Covance, Berkeley, California, USA), anti-Arx1[32] 1:2,000, anti-Nmd3[58] 1:5,000, polyclonal rabbit anti-Mex67 1:5,000 (gift from Catherine Dargemont), anti-Mtr2[59] 1:500, anti-Rpl3[60] 1:4,000, anti-Rei1[25] 1:5,000, anti-CBP 1:2,000 (Cat.-No. CAB1001, Thermo Scientific Open Biosystems, Rockford, Illinois, USA), goat-anti-mouse 1:6,000 (Cat.-No. 170-6516) and mouse-anti-rabbit horse radish peroxidase conjugated antibodies 1:6,000 (Cat.-No. 170-6515, both BIORAD, Munich, Germany). Page Ruler Unstained Protein Ladder (Thermo Scientific, Rockford, Illinois, USA) was used as a protein marker, Brillant Blue G-Colloidal Concentrate Electrophoresis Reagent (Sigma-Aldrich, Munich, Germany) was used for Coomassie stain, and 4-12% NuPAGE Bis-Tris Gels (Novex, Darmstadt, Germany) together with NuPAGE MOPS SDS Running Buffer (Invitrogen, Darmstadt, Germany) were used for SDS-PAGE.

Supplementary Material

Refer to Web version on PubMed Central for supplementary material.

Acknowledgments

We are very thankful to the EMBL-Heidelberg for providing the EM facility and computational infrastructure without which this work would not have been possible, and especially M. Diepholz, C. Blachiere-Batisse, J. Briggs, F. Thommen, and M. Wahlers for advice and technical support. The plasmid pFA6a-HTpA-HIS3MX4 was a kind gift of D. Kressler (Unit of Biochemistry, Department of Biology, University of Fribourg, Fribourg, Switzerland). We thank C. Dargemont (Institut Jacques Monod, Universités Paris VI and VII, Centre National de la Recherche Scientifique, Paris, France), A. W. Johnson (Molecular Genetics & Microbiology, The University of Texas at

Austin, Austin, Texas, USA), A. Lebreton (Unité des Interactions Bactéries-Cellules, Institut Pasteur, Paris, France), and J. R. Warner (Department of Cell Biology, Albert Einstein College of Medicine of Yeshiva University, Bronx, New York, USA) for providing antibodies. This work was supported by grants from the Wellcome Trust (D.T.) and the Deutsche Forschungsgemeinschaft (DFG Hu363/10-4 to E.H.).

REFERENCES

1. Kressler D, Hurt E, Bassler J. Driving ribosome assembly. Biochim Biophys Acta. 2010; 1803:673–83. [PubMed: 19879902]
2. Karbstein K. Inside the 40S ribosome assembly machinery. Curr Opin Chem Biol. 2011; 15:657–63. [PubMed: 21862385]
3. Gorlich D, Kutay U. Transport between the cell nucleus and the cytoplasm. Annual review of cell and developmental biology. 1999; 15:607–60.
4. Zemp I, Kutay U. Nuclear export and cytoplasmic maturation of ribosomal subunits. FEBS Lett. 2007; 581:2783–93. [PubMed: 17509569]
5. Spahn CM, et al. Structure of the 80S ribosome from Saccharomyces cerevisiae--tRNA-ribosome and subunit-subunit interactions. Cell. 2001; 107:373–86. [PubMed: 11701127]
6. Armache JP, et al. Cryo-EM structure and rRNA model of a translating eukaryotic 80S ribosome at 5.5-A resolution. Proc Natl Acad Sci U S A. 2010; 107:19748–53. [PubMed: 20980660]
7. Ben-Shem A, Jenner L, Yusupova G, Yusupov M. Crystal structure of the eukaryotic ribosome. Science. 2010; 330:1203–9. [PubMed: 21109664]
8. Rabl J, Leibundgut M, Ataide SF, Haag A, Ban N. Crystal structure of the eukaryotic 40S ribosomal subunit in complex with initiation factor 1. Science. 2011; 331:730–6. [PubMed: 21205638]
9. Klinge S, Voigts-Hoffmann F, Leibundgut M, Arpagaus S, Ban N. Crystal structure of the eukaryotic 60S ribosomal subunit in complex with initiation factor 6. Science. 2011; 334:941–8. [PubMed: 22052974]
10. Tschochner H, Hurt E. Pre-ribosomes on the road from the nucleolus to the cytoplasm. Trends Cell Biol. 2003; 13:255–63. [PubMed: 12742169]
11. Schafer T, et al. Hrr25-dependent phosphorylation state regulates organization of the pre-40S subunit. Nature. 2006; 441:651–5. [PubMed: 16738661]
12. Strunk BS, et al. Ribosome assembly factors prevent premature translation initiation by 40S assembly intermediates. Science. 2011; 333:1449–53. [PubMed: 21835981]
13. Nissan TA, et al. A pre-ribosome with a tadpole-like structure functions in ATP-dependent maturation of 60S subunits. Mol Cell. 2004; 15:295–301. [PubMed: 15260980]
14. Ulbrich C, et al. Mechanochemical removal of ribosome biogenesis factors from nascent 60S ribosomal subunits. Cell. 2009; 138:911–22. [PubMed: 19737519]
15. Ho JH, Kallstrom G, Johnson AW. Nmd3p is a Crm1p-dependent adapter protein for nuclear export of the large ribosomal subunit. J Cell Biol. 2000; 151:1057–66. [PubMed: 11086007]
16. Gadal O, et al. Nuclear export of 60s ribosomal subunits depends on Xpo1p and requires a nuclear export sequence-containing factor, Nmd3p, that associates with the large subunit protein Rpl10p. Mol Cell Biol. 2001; 21:3405–15. [PubMed: 11313466]
17. Sengupta J, et al. Characterization of the nuclear export adaptor protein Nmd3 in association with the 60S ribosomal subunit. J Cell Biol. 2010; 189:1079–86. [PubMed: 20584915]
18. Yao W, et al. Nuclear export of ribosomal 60S subunits by the general mRNA export receptor Mex67-Mtr2. Mol Cell. 2007; 26:51–62. [PubMed: 17434126]
19. Yao W, Lutzmann M, Hurt E. A versatile interaction platform on the Mex67-Mtr2 receptor creates an overlap between mRNA and ribosome export. EMBO J. 2008; 27:6–16. [PubMed: 18046452]
20. Bradatsch B, et al. Arx1 functions as an unorthodox nuclear export receptor for the 60S preribosomal subunit. Mol Cell. 2007; 27:767–79. [PubMed: 17803941]
21. Hung NJ, Lo KY, Patel SS, Helmke K, Johnson AW. Arx1 is a nuclear export receptor for the 60S ribosomal subunit in yeast. Mol Biol Cell. 2008; 19:735–44. [PubMed: 18077551]
22. Yao Y, et al. Ecm1 is a new pre-ribosomal factor involved in pre-60S particle export. RNA. 2010; 16:1007–17. [PubMed: 20348449]

23. Oeffinger M, Dlakic M, Tollervey D. A pre-ribosome-associated HEAT-repeat protein is required for export of both ribosomal subunits. Genes Dev. 2004; 18:196–209. [PubMed: 14729571]
24. Hackmann A, Gross T, Baierlein C, Krebber H. The mRNA export factor Npl3 mediates the nuclear export of large ribosomal subunits. EMBO Rep. 2011; 12:1024–31. [PubMed: 21852791]
25. Lebreton A, et al. A functional network involved in the recycling of nucleocytoplasmic pre-60S factors. J Cell Biol. 2006; 173:349–60. [PubMed: 16651379]
26. Nissan TA, Bassler J, Petfalski E, Tollervey D, Hurt E. 60S pre-ribosome formation viewed from assembly in the nucleolus until export to the cytoplasm. EMBO J. 2002; 21:5539–47. [PubMed: 12374754]
27. Ben-Shem A, et al. The structure of the eukaryotic ribosome at 3.0 A resolution. Science. 2011; 334:1524–9. [PubMed: 22096102]
28. Kowalinski E, et al. The crystal structure of Ebp1 reveals a methionine aminopeptidase fold as binding platform for multiple interactions. FEBS Lett. 2007; 581:4450–4. [PubMed: 17765895]
29. Monie TP, et al. Structural insights into the transcriptional and translational roles of Ebp1. EMBO J. 2007; 26:3936–44. [PubMed: 17690690]
30. Gartmann M, et al. Mechanism of eIF6-mediated inhibition of ribosomal subunit joining. J Biol Chem. 2010; 285:14848–51. [PubMed: 20356839]
31. Groft CM, Beckmann R, Sali A, Burley SK. Crystal structures of ribosome anti-association factor IF6. Nature structural biology. 2000; 7:1156–64.
32. Lebreton A, Saveanu C, Decourty L, Jacquier A, Fromont-Racine M. Nsa2 is an unstable, conserved factor required for the maturation of 27 SB pre-rRNAs. J Biol Chem. 2006; 281:27099–108. [PubMed: 16861225]
33. Granneman S, Petfalski E, Tollervey D. A cluster of ribosome synthesis factors regulate pre-rRNA folding and 5.8S rRNA maturation by the Rat1 exonuclease. EMBO J. 2011; 30:4006–19. [PubMed: 21811236]
34. Granneman S, Petfalski E, Swiatkowska A, Tollervey D. Cracking pre-40S ribosomal subunit structure by systematic analyses of RNA-protein cross-linking. EMBO J. 2010; 29:2026–36. [PubMed: 20453830]
35. Granneman S, Kudla G, Petfalski E, Tollervey D. Identification of protein binding sites on U3 snoRNA and pre-rRNA by UV cross-linking and high-throughput analysis of cDNAs. Proc Natl Acad Sci U S A. 2009; 106:9613–8. [PubMed: 19482942]
36. Beckmann R, et al. Architecture of the protein-conducting channel associated with the translating 80S ribosome. Cell. 2001; 107:361–72. [PubMed: 11701126]
37. Sweeney R, Chen L, Yao MC. An rRNA variable region has an evolutionarily conserved essential role despite sequence divergence. Molecular and cellular biology. 1994; 14:4203–15. [PubMed: 8196658]
38. Wilson DN, Nierhaus KH. Ribosomal proteins in the spotlight. Crit Rev Biochem Mol Biol. 2005; 40:243–67. [PubMed: 16257826]
39. Kemmler S, Occhipinti L, Veisu M, Panse VG. Yvh1 is required for a late maturation step in the 60S biogenesis pathway. The Journal of cell biology. 2009; 186:863–80. [PubMed: 19797079]
40. Lo KY, Li Z, Wang F, Marcotte EM, Johnson AW. Ribosome stalk assembly requires the dual-specificity phosphatase Yvh1 for the exchange of Mrt4 with P0. The Journal of cell biology. 2009; 186:849–62. [PubMed: 19797078]
41. Kruiswijk T, Planta RJ, Krop JM. The course of the assembly of ribosomal subunits in yeast. Biochim Biophys Acta. 1978; 517:378–89. [PubMed: 626744]
42. Bassler J, Kallas M, Hurt E. The NUG1 GTPase reveals and N-terminal RNA-binding domain that is essential for association with 60 S pre-ribosomal particles. The Journal of biological chemistry. 2006; 281:24737–44. [PubMed: 16803892]
43. Hung NJ, Johnson AW. Nuclear recycling of the pre-60S ribosomal subunit-associated factor Arx1 depends on Rei1 in Saccharomyces cerevisiae. Mol Cell Biol. 2006; 26:3718–27. [PubMed: 16648468]
44. Hedges J, West M, Johnson AW. Release of the export adapter, Nmd3p, from the 60S ribosomal subunit requires Rpl10p and the cytoplasmic GTPase Lsg1p. EMBO J. 2005; 24:567–79. [PubMed: 15660131]

45. Strunk BS, Novak MN, Young CL, Karbstein K. A translation-like cycle is a quality control checkpoint for maturing 40S ribosome subunits. Cell. 2012; 150:111–21. [PubMed: 22770215]
46. Thomson E, Tollervey D. The final step in 5.8S rRNA processing is cytoplasmic in Saccharomyces cerevisiae. Mol Cell Biol. 2010; 30:976–84. [PubMed: 20008552]
47. Becker T, et al. Structure of monomeric yeast and mammalian Sec61 complexes interacting with the translating ribosome. Science. 2009; 326:1369–73. [PubMed: 19933108]
48. DeLano, WL. The PyMOL Molecular Graphics System. 2002. http://www.pymol.org
49. Puig O, et al. The tandem affinity purification (TAP) method: a general procedure of protein complex purification. Methods. 2001; 24:218–29. [PubMed: 11403571]
50. Longtine MS, et al. Additional modules for versatile and economical PCR-based gene deletion and modification in Saccharomyces cerevisiae. Yeast. 1998; 14:953–61. [PubMed: 9717241]
51. Ludtke SJ, Baldwin PR, Chiu W. EMAN: semiautomated software for high-resolution single-particle reconstructions. J Struct Biol. 1999; 128:82–97. [PubMed: 10600563]
52. van Heel M, Harauz G, Orlova EV, Schmidt R, Schatz M. A new generation of the IMAGIC image processing system. J Struct Biol. 1996; 116:17–24. [PubMed: 8742718]
53. Radermacher M, Wagenknecht T, Verschoor A, Frank J. Three-dimensional reconstruction from a single-exposure, random conical tilt series applied to the 50S ribosomal subunit of Escherichia coli. J Microsc. 1987; 146:113–36. [PubMed: 3302267]
54. Frank J, et al. SPIDER and WEB: processing and visualization of images in 3D electron microscopy and related fields. J Struct Biol. 1996; 116:190–9. [PubMed: 8742743]
55. Pettersen EF, et al. UCSF Chimera--a visualization system for exploratory research and analysis. J Comput Chem. 2004; 25:1605–12. [PubMed: 15264254]
56. Wagenknecht T, Grassucci R, Frank J. Electron microscopy and computer image averaging of ice-embedded large ribosomal subunits from Escherichia coli. J Mol Biol. 1988; 199:137–47. [PubMed: 2451023]
57. Penczek PA, Frank J, Spahn CM. A method of focused classification, based on the bootstrap 3D variance analysis, and its application to EF-G-dependent translocation. Journal of structural biology. 2006; 154:184–94. [PubMed: 16520062]
58. Ho JH, Kallstrom G, Johnson AW. Nascent 60S ribosomal subunits enter the free pool bound by Nmd3p. RNA. 2000; 6:1625–34. [PubMed: 11105761]
59. Santos-Rosa H, et al. Nuclear mRNA export requires complex formation between Mex67p and Mtr2p at the nuclear pores. Molecular and cellular biology. 1998; 18:6826–38. [PubMed: 9774696]
60. Vilardell J, Warner JR. Ribosomal protein L32 of Saccharomyces cerevisiae influences both the splicing of its own transcript and the processing of rRNA. Mol Cell Biol. 1997; 17:1959–65. [PubMed: 9121443]

Europe PMC Funders Author Manuscripts

Europe PMC Funders Author Manuscripts

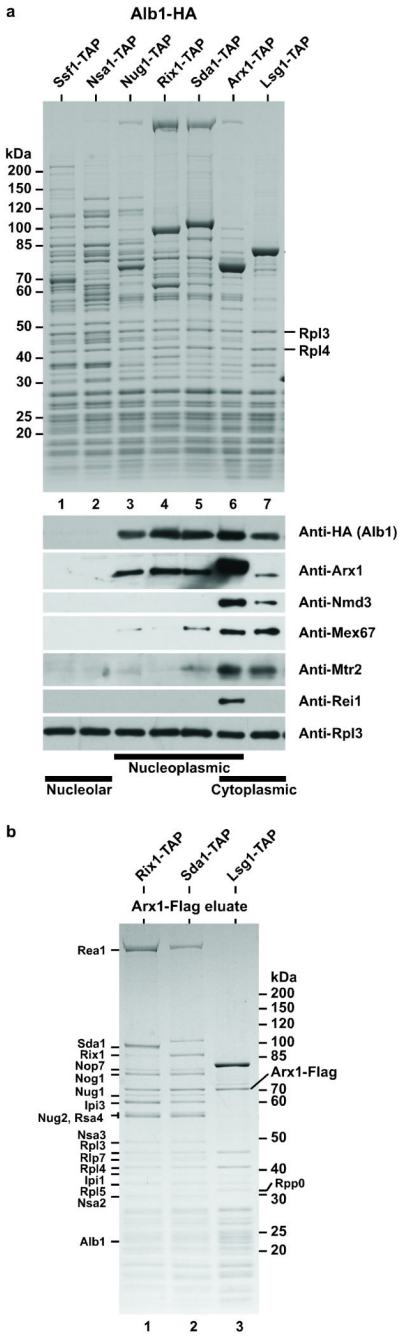

Figure 1. Arx1 and Alb1 are present on the same pre-60S particles

(**a**) Tandem affinity purification of different pre-60S particles (nucleolar, nucleoplasmic, cytoplasmic) using the indicated TAP-tagged bait proteins from the respective yeast strains harboring chromosomally integrated Alb1-HA. The final eluates of these purifications were analyzed by SDS-PAGE and Coomassie staining (upper panel), or Western blotting (lower panel) using the indicated antibodies against pre-ribosomal factors and r-proteins. The position of the respective Coomassie-stained TAP-tagged bait protein is marked by a star. A protein marker is indicated on the left, the position of two r-proteins (Rpl3, Rpl4) on the right, and the subcellular location of the purified particles below.

(**b**) Split-tag affinity purification reveals Arx1 as a stoichiometric factor both on nucleoplasmic and cytoplasmic pre-60S particles. Arx1-containing pre-60S particles were affinity-purified via the split-tag method using the indicated Rix1-TAP, Sda1-TAP and Lsg1-TAP bait proteins with integrated Arx1-Flag. It was first purified on IgG-beads exploiting the ProtA-tag, followed by purification of the TEV-eluate on Flag-beads using co-enriched Arx1-Flag as affinity-ligand. The final eluates obtained after Flag peptide elution were analyzed by SDS-PAGE and Coomassie staining. Indicated are the position of Arx1-Flag, Alb1 and other prominent biogenesis factors on the right and left, respectively, the TAP-tagged bait proteins by a star, and a protein marker on the right.

Europe PMC Funders Author Manuscripts

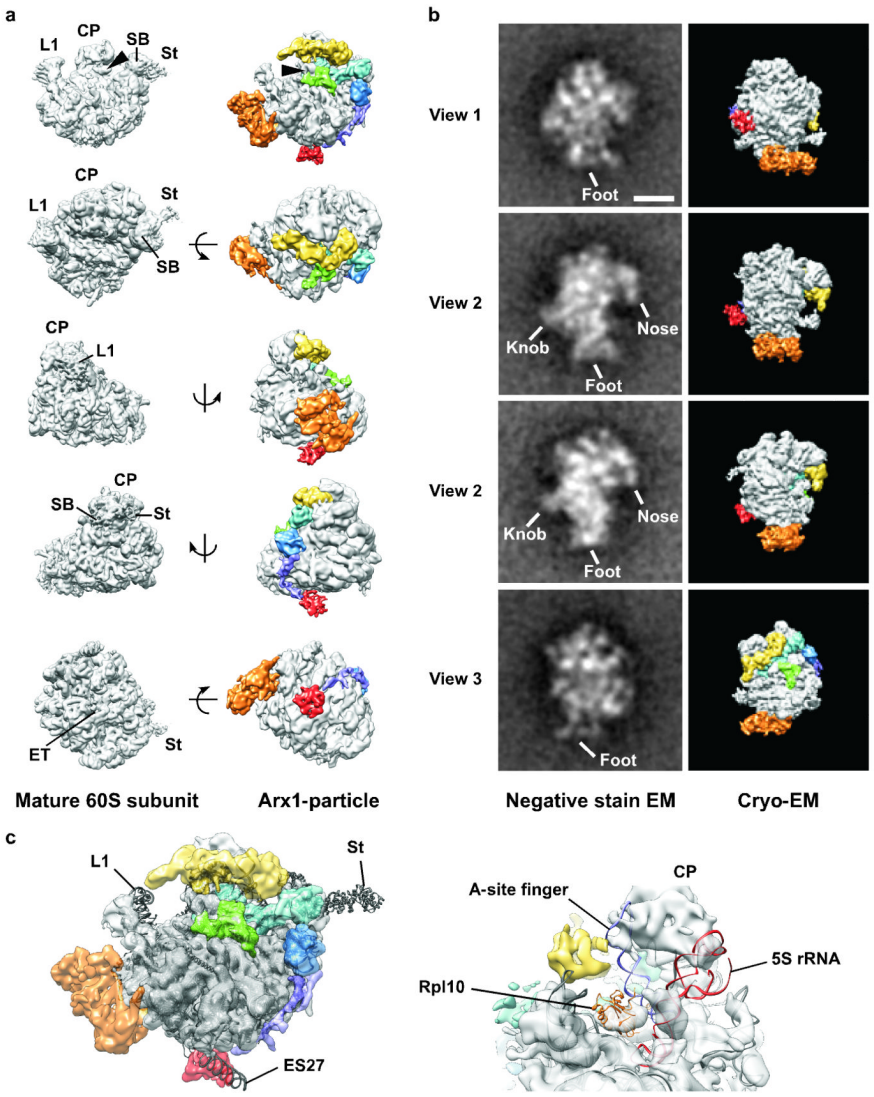

Figure 2. Cryo-EM reconstruction of the Arx1-particle

(**a**) Cryo-EM reconstruction of the Alb1-TAP affinity-purified pre-60S at 11.9 Å resolution (right) in comparison to mature 60S subunit, isolated from *S. cerevisiae* RNC-Ssh1[47] (left). Labeled are: L1-stalk (L1), central protuberance (CP), stalk base (SB), P-stalk (St), exit tunnel (ET). The pre-60S contains additional masses located near the exit tunnel (red), below the L1-stalk (orange), around the central protuberance (yellow), in the center of the inter-subunit surface (green), next to the stalk base (cyan and blue), in the P-site (cyan), and between below the stalk base and exit tunnel region (purple). The crown view (upper panel) is rotated by 90° as indicated. Arrowheads indicate helix 69.

(**b**) Comparison of the Arx1-particle reconstruction (right) with negative stain EM class averages (left) both affinity-purified via Alb1-TAP at 5 mM $MgCl_2$. Colors as in **a**. Characteristic pre-ribosomal structures of the Arx1-particle are labeled (*foot*, orange; *nose*, yellow and parts of the central protuberance; *knob*, red). Scale bar, 10 nm.

(**c**) A 60S subunit model containing ES27 in *out* conformation (ribbon; PDB: 3IZF, 3IZD, 3IZS[6]) was fitted into the Arx1-particle reconstruction. The close-up (right) is displayed at higher contour level than the overview (left). In most areas the model fits well into the density (left). No density was observed for the mature positions of A-site finger (purple) and

5S rRNA (red; right). The density found at the mature location of Rpl10 (orange) does not fit its shape and displays typical features of RNA density. Abbreviations as in **a**.

Europe PMC Funders Author Manuscripts

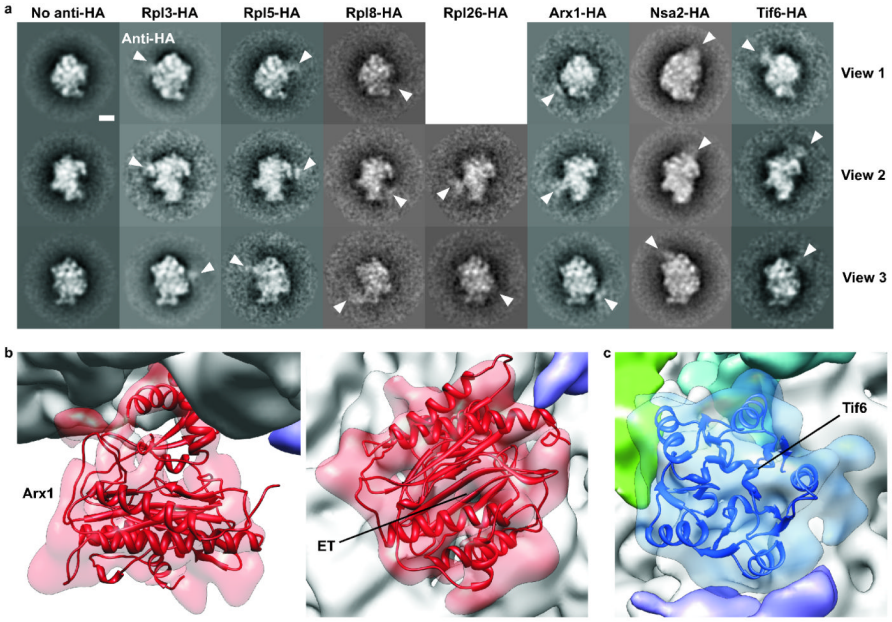

Figure 3. Immuno-EM reveals the relative position of biogenesis factors and r-proteins on the Arx1-particle

(**a**) Class averages of negative-stained Arx1-particles affinity-purified via Alb1-TAP with anti-HA antibody bound to the indicated C-terminally integrated HA-tagged proteins of interest. The three typical orientations of the Arx1-particle are depicted (view 1–3). The white arrow heads indicate the antibody-derived extra density as compared to control Arx1-particle (Alb1-TAP with integrated Arx1-HA) without added antibody (no anti-HA). Scale bar, 10 nm.

(**b**) Arx1 localizes to the *knob* structure of the Arx1-particle, as shown by immuno-labeling in **a**. Ebp1, the slightly smaller human homolog of Arx1, resembles the *knob* structure of the Arx1-particle in size and shape. The crystal structure of Ebp1 (red ribbon; PDB: 2Q8K[28]) was fitted into the cryo-EM density attributed to Arx1 (red surface). According to this fit, the Arx1 binding pocket would be facing towards the pre-60S subunit, but it would not be occluded. The fit is shown according to the crown (left) and bottom views (right) of the particle. Colors and abbreviations as in Fig. 2a.

(**c**) The additional mass colored in blue matches the ribosomal anti-association factor Tif6 in position, size, and shape. The crystal structure of Tif6 (blue ribbon; PDB: 1G62[31]) fits well into the blue density. Colors as in Fig. 2a.

Europe PMC Funders Author Manuscripts

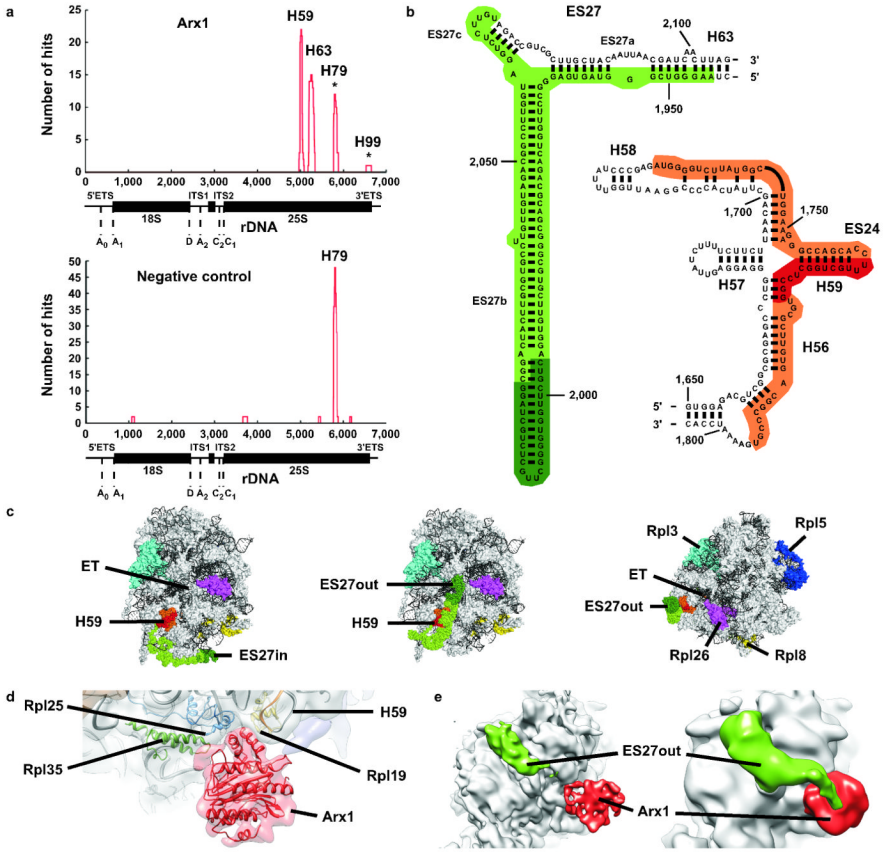

Figure 4. CRAC analysis confirms the location of Arx1 near the exit tunnel

(**a**) CRAC analysis on Arx1-HTP and untagged strain. Total number of hits plotted against the relative location along the rDNA sequence. Arx1 binds helix 59 (H59; 22 hits) and helix 63 (15 hits; upper panel). Peaks marked by an asterisk also appear in the negative control (lower panel).

(**b**) Arx1 positioning in a 25S rRNA model (adapted from ref. 6). Nucleotides found in all hits (peak tips in **a**): dark green, red; nucleotides found in both experiments: green, orange. ES27 on helix 63 comprises three arms (ES27a–c), ES24 is an extension of helix 59.

(**c**) Arx1 binding presented in a 60S model (PDB: 3IZS, 3IZF, 3IZD[6], displayed using PyMOL[48]). rRNA, gray; r-proteins, light gray; Rpl5, blue; Rpl3, cyan; Rpl26, magenta; Rpl8, yellow. Nucleotides bound by Arx1 colored as in **b**. ES27 was described in two conformations[6]. The ES27*out* conformation (middle, right) brings the main cross-links (red, dark green) close together nearby the exit tunnel (ET), contrary to the ES27*in* conformation (left).

(**d**) A 60S model (PDB: 3O58[7]) and Ebp1 (see Fig. 3b) were fitted into our Arx1-particle reconstruction. The Arx1-density contacts the subunit close to helix 59 (orange nucleotides red in **b**), Rpl25 (blue) and Rpl35 (green). Rpl19 (yellow) is nearby. Colors as Fig. 2a.

(**e**) Arx1 (red) contacts ES27 (green) in its *out* conformation. The Arx1-particle (grey) is shown at contour level 0.45 (left; as Fig. 2a) and 0.06 (right; low-pass filtered between 17–19 Å).

Europe PMC Funders Author Manuscripts

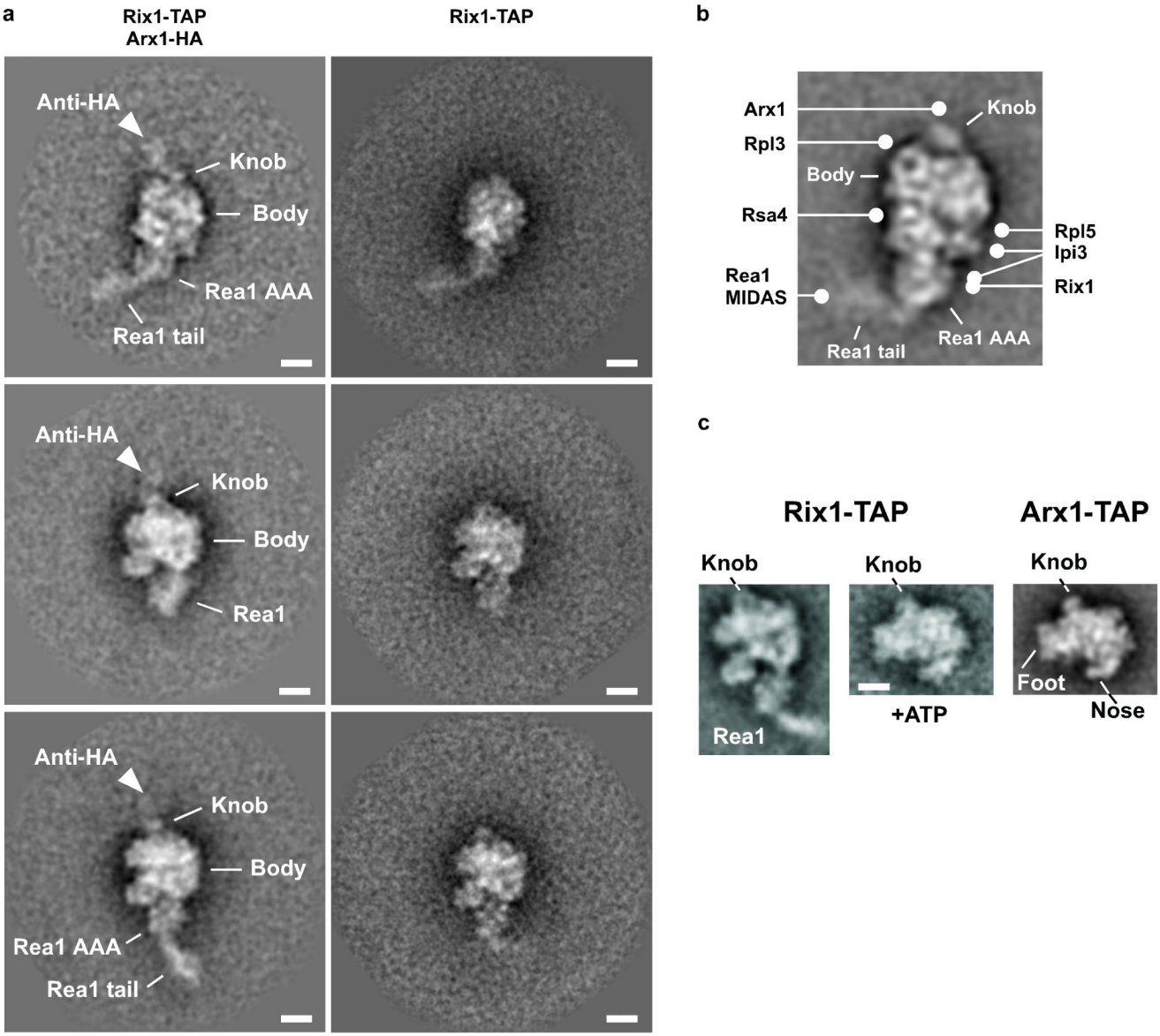

Figure 5. Arx1 localizes to the *knob* structure of the Rix1-particle, a precursor of the Arx1-particle

(**a**) Immuno-EM analysis reveals the position of Arx1 on the Rix1-particle. Rix1-TAP was affinity-purified in the presence of an anti-HA antibody from a strain with genomically integrated Arx1-HA (left panel) or with no HA integration (right panel). The Rix1-particles were analyzed by negative stain EM and single particle analysis, and three typical class averages are shown. The main structural features of the Rix1-particle are indicated as "body", "Rea1 AAA" (AAA^+ ATPase ring), "Rea1 tail" and "knob". The white arrow points to the additional mass attributed to the bound anti-HA antibody and indicative of the position of Arx1 on the particle. Scale bar, 10 nm.

(**b**) Arx1 localizes to the conspicuous *knob* structure of the Rix1-particle. The position of Arx1 is shown in relation to the known positions of Rpl3, Rsa4, Rpl5, Ipi3, Rix1, and Rea1-MIDAS determined by immuno-EM on the Rix1-particle (adapted to ref. 14). The "body", "knob", "Rea1 AAA", and "Rea1-MIDAS" are indicated as main features of the Rix1-particle.

(**c**) Comparison of Rix1-particle and Arx1-particle class averages. Comparison of Rix1-TAP particles containing the Rea1-tail and tail-less particles obtained after ATP-treatment (+ATP; adapted from Supplementary Fig. 1a, see ref. 14), and particles affinity-purified via Arx1-TAP. In all cases, the typical “knob” is indicated. Scale bar, 10 nm.

Europe PMC Funders Author Manuscripts